J Therm Anal Calorim (2010) 101:137–142
DOI 10.1007/s10973-009-0557-7

Cation distribution in manganese cobaltite spinels $Co_{3-x}Mn_xO_4$ ($0 \leq x \leq 1$) determined by thermal analysis

H. Bordeneuve · A. Rousset · C. Tenailleau · S. Guillemet-Fritsch

Received: 10 June 2009 / Accepted: 13 October 2009 / Published online: 3 November 2009

Abstract Thermogravimetric analysis was used in order to study the reduction in air of submicronic powders of $Co_{3-x}Mn_xO_4$ spinels, with $0 \leq x \leq 1$. For $x = 0$ (i.e. Co_3O_4), cation reduction occurred in a single step. It involved the Co^{III} ions at the octahedral sites, which were reduced to Co^{2+} on producing CoO. For $0 < x \leq 1$, the reduction occurred in two stages at increasing temperature with increasing amounts of manganese. The first step corresponded to the reduction of octahedral Co^{III} ions and the second was attributed to the reduction of octahedral Mn^{4+} ions to Mn^{3+}. From the individual weight losses and the electrical neutrality of the lattice, the Co^{III} and Mn^{4+} ion concentrations were calculated. The distribution of cobalt and manganese ions present on each crystallographic site of the spinel was determined. In contrast to most previous studies that took into account either Co^{III} and Mn^{3+} or Co^{2+}, Co^{III} and Mn^{4+} only, our thermal analysis study showed that Co^{2+}/Co^{III} and Mn^{3+}/Mn^{4+} pairs occupy the octahedral sites. These results were used to explain the resistivity measurements carried out on dense ceramics prepared from our powders sintered at low temperature (700–750 °C) in a Spark Plasma Sintering apparatus.

Keywords Thermogravimetric analysis · Cobalt and manganese oxides · Spinels · Cation distribution

H. Bordeneuve · A. Rousset · C. Tenailleau (✉) · S. Guillemet-Fritsch
Institut Carnot CIRIMAT, Universite Paul Sabatier, UMR CNRS 5085, 31062 Toulouse Cedex 9, France
e-mail: tenailleau@chimie.ups-tlse.fr

Introduction

Mixed oxides of cobalt and manganese with a spinel structure, $Co_{3-x}Mn_xO_4$, are key compounds in fields of application such as electronics [1, 2], electrocatalysis [3, 4], transport [5, 6] and magnetic sensors [7].

Although numerous studies have been devoted to manganese-rich phases ($Co_{3-x}Mn_xO_4$ with $x \geq 1.5$) [8–10] and specifically to Co_2MnO_4 [11–13], few have concerned cobalt-rich phases ($0 < x < 1$). The physical and chemical properties of single-phase and stoichiometric materials are closely related to the distribution of cations in the spinel lattice. However, the cation distribution is still poorly defined and most publications, even the most recent [6], describe the composition to be of the $Co^{2+}[Co^{III}Mn^{3+}]O_4^{2-}$ or $Co^{2+}[Co^{2+}Mn^{4+}]O_4^{2-}$ type [1, 14–17]. Only a few studies mention mixed valencies with $Co^{2+}[Co_x^{2+}Co_{2-2x}^{III}Mn_x^{4+}]O_4^{2-}$ ($0 \leq x \leq 1$) [2, 17] and $Co^{2+}[Co_a^{III}Mn_b^{2+}Mn_c^{3+}Mn_d^{4+}]O_4^{2-}$ ($a + b + c + d = 2$; $3a + 2b + 3c + 4d = 6$) [11] for the elements cobalt and manganese, respectively. Thus, it is still difficult to conclude as to the valencies of the cations present at the octahedral sites of the spinel lattice while the general consensus of opinion converges towards complete occupation of the tetrahedral sites by Co^{2+} ions [2, 3, 14, 16]. In addition, the trivalent cobalt at the octahedral sites is thought to be in a "low spin" state, written as Co^{III}, as is the case in Co_3O_4, where the actual composition of the sample is $Co^{2+}[Co_2^{III}]O_4^{2-}$ [18–20].

Over the past decades, some of us [21–23] have shown that the reactivity of transition metal cations in the spinel lattice depends on their coordination number but also on their oxidation state, especially for submicronic phases. Thus, thermoanalytical methods can be particularly useful to help determining the position and the oxidation state of cations in the spinel structure. Thermogravimetric (TG)

analysis applied to manganese cobaltite spinels over the temperature range 25–1,300 °C have thus proved to be very fruitful. The results are described in this article.

Experimental

Preparation

Recently, we reported a method for the preparation of $Co_{3-x}Mn_xO_4$ ($0 \leq x \leq 2$) [24] in powder form. It involved decomposing mixed oxalates of cobalt and manganese $(Co_{1-\alpha}Mn_\alpha)C_2O_4{\cdot}2H_2O$ ($0 \leq \alpha \leq 1$; $x = 3\alpha$) followed by heat treatment in air at 800 °C for 4 h and cooling at 150 °C/h. The compositions studied are reported in Table 1.

Characterization

Phase identification and crystal parameter determination were carried out using X-ray diffraction (XRD) with a Bruker D4 Endeavour, the wavelength being that of the CuKα. Data refinements were performed using the Rietveld method and the Fullprof/Wintplotr program. Crystallite size was determined using a Jeol JSM 6700 F scanning electron microscope fitted with an X-Link energy dispersion analyser, providing concentration data on the Mn and Co present in each sample. The specific surface area measurements were made using the B.E.T. method on a Micrometrics Flowsorb II 2300. The thermal analyses of the oxide powders were performed in air on a Setaram TAG 24 thermobalance, which can record mass variations of 0.1 μg.

Results and discussion

Morphological analysis

The specific surface area "S_w" is plotted versus the composition of $Co_{3-x}Mn_xO_4$ ($0 \leq x \leq 1$) powders heated to 800 °C in air for 4 h in Fig. 1. S_w reached a maximum slightly above 10 m^2/g for a manganese concentration of around 0.3. The diameters of the crystallites calculated from these measurements by the expression $d = \frac{6}{\rho S_w}$ (ρ: density = 6.0) are in good agreement with those obtained by SEM observation (inset in Fig. 1) indicating that the powders are not composed of porous particles. The size of the crystallites varied from a few tens of nanometres (for instance, $d = 94$ nm for $x = 0.28$) to a few hundred nanometres ($d = 356$ nm for $x = 0$); so the powders were sufficiently reactive to use the TG method. This was confirmed by microstructural analyses using the SEM images where $42 < d < 114$ nm and $150 < d < 600$ nm for $x = 0.28$ and 0, respectively.

Table 1 $Co_{3-x}Mn_xO_4$ $0 \leq x \leq 1$ powder compositions ($x = 3\alpha$)

α	0	0.02	0.08	0.13	0.20	0.26	0.33
x	0	0.06	0.24	0.40	0.61	0.78	1

Structural analysis

As reported in the phase diagram for the system Co_3O_4–Mn_3O_4 [25], all the powders of $Co_{3-x}Mn_xO_4$ ($0 \leq x \leq 1$) obtained at 800 °C in air showed cubic symmetry and single phase. The variation of the crystal parameters with the composition, as deduced from the XRD data, shows a linear variation that follows Vegard's law (Fig. 2). This can be explained either by the progressive substitution of the octahedral Co^{III} ions by Mn^{3+} ions with a larger radius ($r_{Mn^{3+}} = 0.065\text{nm} > r_{Co^{III}} = 0.053\text{nm}$) or by Co^{2+} and Mn^{4+} ions knowing that $r_{Co^{2+}} = 0.072\text{nm} > r_{Co^{III}} = 0.053\text{nm}$ and that $r_{Mn^{4+}} = r_{Co^{III}} = 0.053\text{nm}$. These two substitution mechanisms $Co^{III} \rightarrow Mn^{3+}$ or $2Co^{III} \rightarrow Mn^{4+} + Co^{2+}$ led us to calculate variations of the crystal parameters that are both close to the experimental variation. These structural data cannot therefore be used to propose a cation distribution in octahedral sites.

Thermogravimetric analysis

Heating

During the thermogravimetric analysis run, reaching 1,300 °C in air, the $Co_{3-x}Mn_xO_4$ ($0 \leq x \leq 1$) powders underwent significant weight loss over 900 °C (Fig. 3). The higher the proportion of manganese, the higher the temperature at which the weight loss occurred (see inset in Fig. 3). The relationship between the reaction temperature and the composition emphasizes the fact that it was

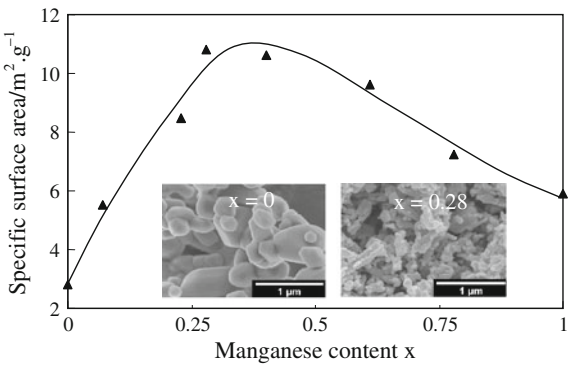

Fig. 1 Specific surface area variation with composition for $Co_{3-x}Mn_xO_4$ powders with $0 \leq x \leq 1$. Inset shows SEM images of powders for $x = 0$ and 0.28. *Scale bar* is 1 μm

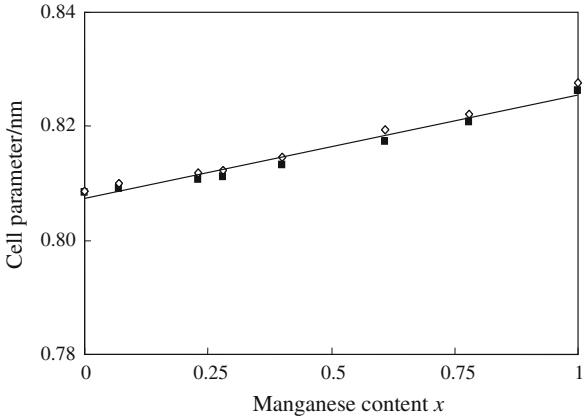

Fig. 2 Cell parameter variation with manganese content for $Co_{3-x}Mn_xO_4$ powders with $0 \leq x \leq 1$. Cell parameters obtained for ceramics are given for comparison (*open symbols*)

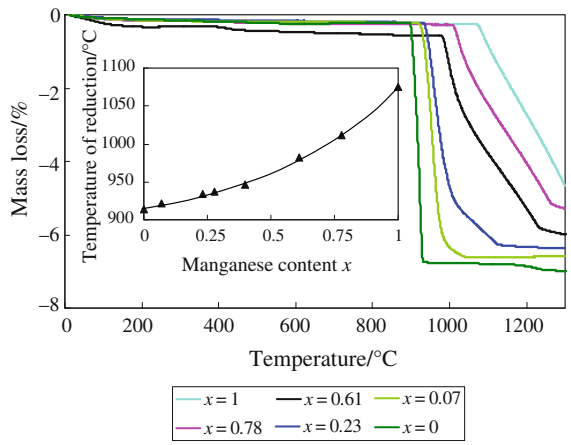

Fig. 3 Mass loss versus temperature for $Co_{3-x}Mn_xO_4$ powders with $0 \leq x \leq 1$ after TG analysis upon heating. Variation of the temperature of reduction with manganese content is given in inset

actually mixed oxides being analyzed and not a mixture of oxides. For $x = 0$, i.e. for Co_3O_4, the weight loss occurred in a single step and over a very short temperature range—just a few degrees. It involved the reduction of the octahedral Co^{III} ions of Co_3O_4 ($Co^{2+}[Co_2^{III}]O_4^{2-}$) into Co^{2+} with formation of CoO following the reaction:

$$Co_3O_4 \rightarrow 3CoO + \frac{1}{2}O_2.$$

The theoretical weight variation due to this reaction is 6.64%, which is very similar to the experimentally determined value of 6.59%. As samples of increasing manganese content were analyzed, the weight loss became slower than for Co_3O_4 and the TG curves started to reveal changes in slope suggesting the reduction of a cation other than Co^{III}. By analogy with the high-temperature behaviour of nickel or copper manganites [26, 27], the second step of the reaction could be attributed to the reduction of unstable

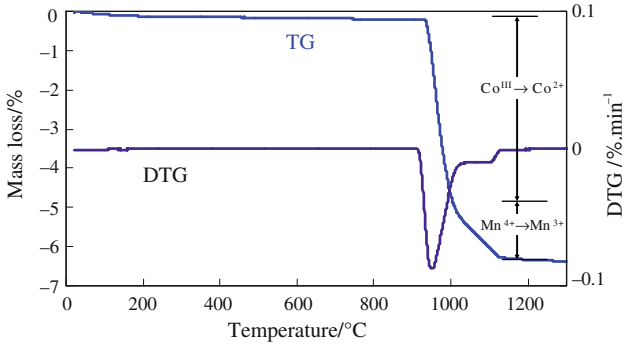

Fig. 4 Mass loss variation versus temperature increase for $Co_{2.77}Mn_{0.23}O_4$ sample powder obtained by TG showing two steps of reduction (also evidenced after derivative DTG analysis)

Mn^{4+} ions in octahedral sites over 1,000 °C yielding Mn^{3+} ions following:

$$MnO_2 \rightarrow \frac{1}{2}Mn_2O_3 + \frac{1}{4}O_2.$$

Thus, the $Co_{3-x}Mn_xO_4$ ($0 < x < 1$) oxides likely undergo reduction of the Co^{III} ions then, at slightly higher temperatures, reduction of the Mn^{4+} ions. An example is given in Fig. 4 showing the TG and DTG curves of the oxide with the composition $Co_{2.77}Mn_{0.23}O_4$.

Like the reduction temperatures, the experimental weight losses resulting from reduction vary with the composition. An almost linear increase of the total weight loss as the proportion of Mn increases is seen in Fig. 5, where we have also plotted the theoretical weight losses calculated for the two cationic distributions usually proposed in the literature. If we first consider the most frequently studied distribution [6, 14, 15], $Co^{2+}[Co_{2-x}^{III}Mn_x^{3+}]O_4^{2-}$ ($0 \leq x \leq 1$), only the Co^{III} ions would be reduced in the temperature range studied. The Mn^{3+} ions are perfectly stable at these temperatures, as proven by the behaviour of Mn_3O_4 ($Mn^{2+}[Mn_2^{3+}]O_4^{2-}$) and that of the manganese-rich $Co_{3-x}Mn_xO_4$ phases ($x > 1.3$) [24]. Here, the weight loss would be lower than the experimental loss, clearly indicating that another cation must also be reduced. The distribution of the elements in this commonly accepted formula, therefore, does not appear to be compatible with our findings.

If we consider a different distribution that is sometimes proposed [2], $Co^{2+}[Co_x^{2+}Co_{2-2x}^{III}Mn_x^{4+}]O_4^{2-}$ ($0 \leq x \leq 1$), the theoretical weight loss affecting the Co^{III} and Mn^{4+} ions is much greater than the experimental loss and varies completely independently of the manganese content. This divergence can be explained by too high a concentration of Mn^{4+} in the distribution considered. One way of lowering the number of Mn^{4+} ions is to introduce manganese at the octahedral sites in an oxidation state of either +2 or +3. As it is known that for compositions with higher proportions of manganese than those studied here ($x > 1.6$), the phases

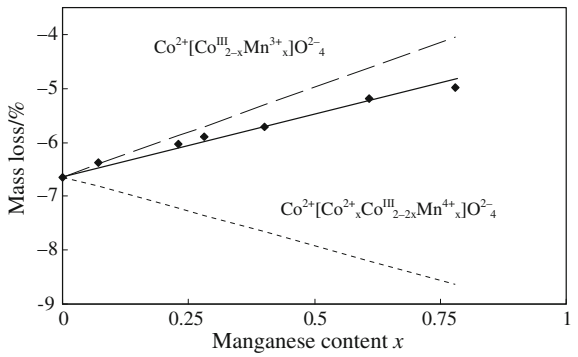

Fig. 5 Total mass loss variation for each composition of $Co_{3-x}Mn_xO_4$ powder ($0 \le x \le 1$) analyzed after heating in TG apparatus up to 1,300 °C. Theoretical mass losses calculated for the two cationic distributions usually proposed in the literature are plotted for comparison (see text for references)

are tetragonal owing to the presence of the Mn^{3+} Jahn–Teller ion, it therefore seems logical to choose the oxidation state +3. A distribution of Co^{2+}, Co^{III}, Mn^{3+} and Mn^{4+} ions on the octahedral sites is thus more suitable to take into account the experimental results for cobalt-rich oxides ($0 < x < 1$).

The concentrations of Co^{III} and Mn^{4+} ions on octahedral sites can be calculated from the weight losses resulting from the reduction reactions recorded on the TG plots. As can be seen in Fig. 6, the concentration of Mn^{4+} ions varies linearly with the composition. Above $x = 0.8$, it is no longer possible to distinguish changes of slope on the TG plots, the reduction of both Co^{III} and Mn^{4+} ions occurring simultaneously. The concentration of Mn^{4+} ions at the *B* sites for $x = 1$ was reached by extrapolation.

From the Mn^{4+} ion concentrations determined experimentally for each composition and the lattice charge neutrality, which requires equal concentrations of Co^{2+} and Mn^{4+}, we were able to calculate the concentrations of Co^{2+}, Mn^{3+} and Co^{III} at the octahedral sites (Table 2). Variations of each ion concentration with the composition

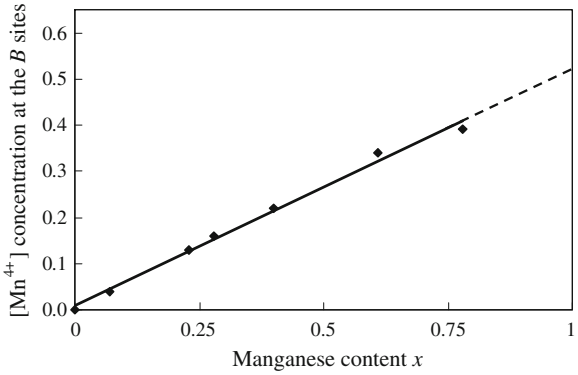

Fig. 6 Variation of Mn^{4+} ion concentration at the B sites with x for $Co_{3-x}Mn_xO_4$ powders, with $0 \le x \le 1$

Table 2 Concentrations of Co^{2+}, Co^{III}, Mn^{3+}, Mn^{4+} ions at the octahedral sites for the $Co_{3-x}Mn_xO_4$ ($0 \le x \le 1$) cubic phases

x	Co^{2+}	Co^{III}	Mn^{3+}	Mn^{4+}
0	0	2	0	0
0.07	0.04	1.89	0.03	0.04
0.23	0.13	1.64	0.10	0.13
0.28	0.16	1.56	0.12	0.16
0.40	0.22	1.38	0.18	0.22
0.61	0.34	1.05	0.27	0.34
0.78	0.39	0.83	0.39	0.39
1	0.53	0.46	0.48	0.53

are given in Fig. 7. The increase in the manganese concentration can be related to a linear decrease in the concentration of Co^{III} ions and to an increase in the concentrations of Mn^{3+}, Co^{2+} and Mn^{4+} ions at the octahedral sites. The concentrations of Co^{2+} and Mn^{4+} ions always remain a little bit higher than those of Mn^{3+} ions.

Cooling

After reaching 1,300 °C, the powders were cooled in air at 2 °C/min. The TG plots in Fig. 8 indicate oxygen uptake and hence the reversible character of the reduction reactions described during heating. Although the oxidation temperatures—with respect to the composition—are symmetrical with the reduction temperatures, the quantity of oxygen taken up is not. With slower cooling, total re-oxidation was approached. For $x = 0$ (CoO), a single oxidation step was observed, while separate partial oxidations of the Mn^{3+} and Co^{2+} ions occurred for mixed oxides. The partial re-oxidation reaction rates were much slower.

Cation distribution

The unusual distribution of the type $Co^{2+}[Co^{2+}_a Co^{III}_b Mn^{3+}_c Mn^{4+}_d]O_4^{2-}$ with $a + b + c + d = 2, 2a + 3b + 3c + 4d = 6$, $a + b = 2 - x$ and $c + d = x$, which was determined from the TG data presents the major characteristic of having a double mixed valency Co^{2+}/Co^{III} and Mn^{3+}/Mn^{4+} over the whole series of composition $Co_{3-x}Mn_xO_4$ ($0 < x < 1$). This distribution can be related to semiconducting properties found for ceramics prepared by Spark Plasma Sintering (SPS) using the powders studied in this article. Variation of resistivity with composition is in agreement with the distribution found from the thermal analysis (Fig. 9). For $x = 1$, i.e. when the number of Co^{2+}/Co^{III} and Mn^{3+}/Mn^{4+} couples was maximum, the resistivity was the lowest ($\rho = 329\ \Omega$ cm) and likewise, when the number of cation couples decreased ($x < 0.4$) the resistivity increased. Distributions of the type $Co^{2+}[Co^{2+}Mn^{4+}]O_4^{2-}$

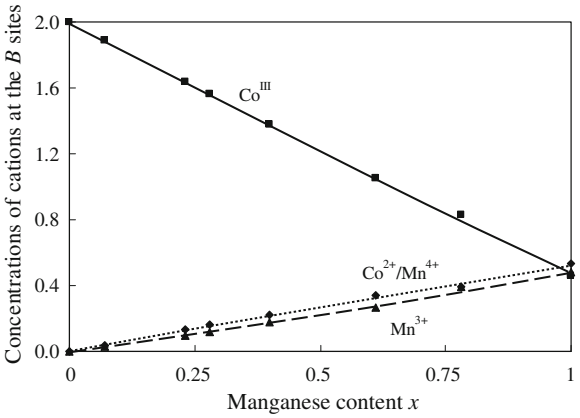

Fig. 7 Variations of cation concentrations for $Co_{3-x}Mn_xO_4$ powders, with $0 \leq x \leq 1$

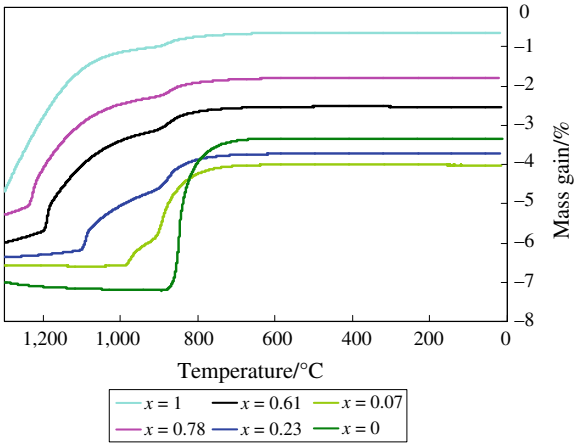

Fig. 8 Mass loss versus temperature for $Co_{3-x}Mn_xO_4$ powders with $0 \leq x \leq 1$ after TG analysis upon cooling

for Co_2MnO_4 ($x = 1$) or $Co^{2+}[Co^{III}_{2-x}Mn^{3+}_x]O_4{}^{2-}$ for $0 \leq x < 1$ cannot provide a valid explanation of the experimentally observed electrical properties. The SPS technique enabled the powders to be compacted in a few minutes at 750 °C, i.e. a temperature lower than that used to prepare them, and grain sizes are often preserved in ceramic products. Cell parameter variations with composition for powders and ceramics are identical (see Fig. 2). Elemental and charge distributions were conserved after SPS treatment. Our current investigations based on neutron diffraction data of cobalt and manganese oxide spinel ceramics tend to confirm the cation distributions determined after TG measurements.

Conclusions

Applying thermogravimetric analysis to submicronic $(Co_{3-x}Mn_x)O_4$ ($0 \leq x \leq 1$) powders obtained at 800 °C

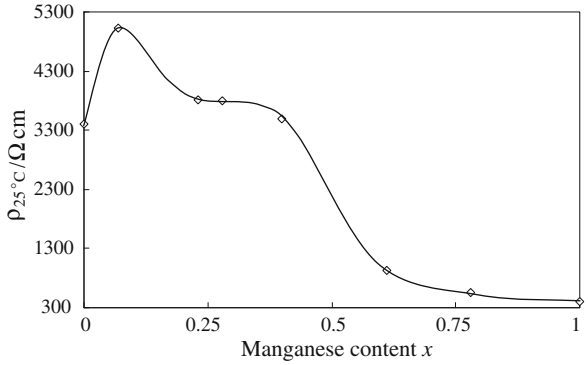

Fig. 9 Resistivity variation versus composition for $Co_{3-x}Mn_xO_4$ ceramics with $0 \leq x \leq 1$

indicated the occurrence of distinct oxidation–reduction phenomena with two steps of transformation involving the couples Co^{2+}/Co^{III} and Mn^{3+}/Mn^{4+}. TG data analyses provided the cation distribution for each composition of the corresponding cubic spinel. This distribution, written as $Co^{2+}[Co^{2+}_a Co^{III}_b Mn^{3+}_c Mn^{4+}_d]O_4{}^{2-}$ and characterized by the presence of a double mixed valency at the octahedral sites, can justify the semiconducting properties observed in ceramics. The novel cation distribution proposed here can explain the electron conduction that occurs in $Co_{3-x}Mn_xO_4$ spinel ceramics through a polaron hopping mechanism between pairs of Co^{2+}/Co^{III} and Mn^{3+}/Mn^{4+} ions positioned at the octahedral sites.

Acknowledgements The authors wish to thank the Vishay BCcomponents Company based in Belgium for financial support.

References

1. Kolomiets BT, Sheftel J, Kurlina E. Electrical properties of some compound oxide semiconductors. Sov Phys Tech Phys. 1957;2: 40–58.
2. Jabry EH, Rousset A, Lagrange A. Preparation and characterization of manganese and cobalt based semiconducting ceramics. Phase Transit. 1988;13:63–71.
3. Rios E, Gautier JL, Poillerat G, Chartier P. Mixed valency spinel oxides of transition metals and electrocatalysis : case of the $Mn_xCo_{3-x}O_4$ system. Electrochim Acta. 1998;44:1491–7.
4. Restovic A, Rios E, Barbato S, Ortiz J, Gautier JL. Oxygen reduction in alkaline medium at thin $Mn_xCo_{3-x}O_4$ ($0 \leq x \leq 1$) spinel films prepared by spray pyrolysis. Effect of oxide cation composition on the reaction kinetics. J Electroanal Chem. 2002;522:141–51.
5. Yang Z, Xia GG, Li XH, Stevenson JW. (Mn, Co)3O_4 spinel coatings on ferritic stainless steels for SOFC interconnect applications. Int J Hydrogen Energy. 2006;32:3648–54.
6. Hagen A, Mikkelsen L. Xanes study of the oxidation state and coordination environment of manganese, chromium and cobalt in spinel type materials. Proceedings of the 26th Risø international symposium on material science: Solid State Electrochem 2005; p. 197–202.

7. Philip J, Kutty TRN. Colossal magnetoresistance of oxide spinels $Co_xMn_{3-x}O_4$. Mater Lett. 1999;39:311–7.
8. Buhl R. Manganites spinelles purs d'éléments de transition préparations et structures cristallographiques. J Phys Chem Solids. 1969;30:805–12.
9. Martin de Vidales JL, Vila E, Rojas RM, Garcia-Martinez D. Thermal behavior in air and reactivity in acid medium of cobalt manganese spinels $Mn_xCo_{3-x}O_4$ ($1 \leq x \leq 3$) synthesized at low temperature. Chem Mater. 1995;7:1716–21.
10. Boucher B, Buhl R, Perrin M. Magnetic structure of cobalt manganite by neutron diffraction. J Appl Phys. 1968;39:632–4.
11. Gautier JL, Cabezas C, Barbato S. Réduction électrochimique de $MnCo_2O_4$ préparé à basse et haute température. Electrochim Acta. 1981;26:1377–82.
12. Vasil'ev GP, Pakhomov LA, Ryabova LA. Structural and electrical properties of d.c. sputtered $MnCo_2O_4$ films. Thin Solid Films. 1980;66:119–24.
13. Borges FMM, Melo DMA, Camara MSA, Martinelli AE, Soares V, de Araujo JH, et al. Magnetic behavior of nanocristalline $MnCo_2O_4$ spinels. J Magn Magn Mater. 2006;302:273–7.
14. Boucher B, Buhl R, Di Bella R, Perrin M. Etude par des mesures de diffraction de neutrons et de magnétisme des propriétés cristallines et magnétiques de composés cubiques spinelles $Co_{3-x}Mn_xO_4$ (0, $6 \leq x \leq 1$, 2). J Phys. 1970;31:113–9.
15. Naka S, Inagaki M, Tanaka T. On the formation of solid solution in $Co_{3-x}Mn_xO_4$ system. J Mater Sci. 1972;7:441–4.
16. Wickham DG, Croft WJ. Crystallographic and magnetic properties of several spinels containing trivalent manganese. J Phys Chem Solids. 1958;7:351–60.
17. Aoki J. Tetragonal distorsion of the oxide Spinels containing cobalt and manganese. J Phys Soc Jpn. 1962;17:53–61.
18. Gorter EW. Saturation magnetization and crystal chemistry of ferrimagnetic oxides. I. II. Theory of ferrimagnetism. Philips Res Rep. 1954;9:295–365.
19. Cossee P. Structure and magnetic properties of Co_3O_4 and $ZnCo_2O_4$. Recl Trav Chim Pays-Bas Belg. 1956;75:1089–96.
20. Roth WL. The magnetic structure of Co_3O_4. J Phys Chem Solids. 1964;25:1–10.
21. Rousset A, Clerc L, Vajpei AC, Gillot B, Jemmali F. Thermoanalytical studies on cation distribution in submicronic titanomagnetites. J Therm Anal Cal. 1987;32:845–55.
22. Rousset A, Tailhades Ph, Gillot B. Relations structure-réactivité dans des ferrites submicroniques à valence mixte. Ann Chim Fr. 1989;14:187–99.
23. Domenichini B, Gillot B, Tailhades Ph, Bouet L, Rousset BA, Perriat P. Cationic distribution and oxidation kinetics of trivalent molybdenum ions in submicron molybdenum substituted magnetites. Solid State Ion. 1992;58:61–9.
24. Bordeneuve H, Guillemet-Fritsch S, Rousset A, Schuurman S, Poulain V. Structure and electrical properties of single phase cobalt manganese oxide spinels $Mn_{3-x}Co_xO_4$ sintered classically and by Spark Plasma Sintering. J Solid State Chem. 2009;182:396–401.
25. Aukrust E, Muan A. Thermodynamic properties of solid solutions with spinel type structure. The system Co_3O_4–Mn_3O_4. Trans Metall Soc AIME. 1964;230:378–82.
26. Rousset A, Lagrange A, Brieu M, Couderc JJ, Legros R. Influence de la microstructure sur la stabilité électrique des thermistances CTN. J Phys III. 1993;3:833–45.
27. Brieu M, Couderc JJ, Rousset A, Legros RJ. TEM characterization of nickel and nickel–cobalt manganite ceramics. Eur Ceram Soc. 1993;11:171–7.